JOURNAL OF MAGNETIC RESONANCE **130,** 346–351 (1998)
ARTICLE NO. MN971312

# Quantitative Investigation of Dipole–CSA Cross-Correlated Relaxation by ZQ/DQ Spectroscopy

B. Brutscher, N. R. Skrynnikov, T. Bremi, R. Brüschweiler, and R. R. Ernst

*Laboratorium für Physikalische Chemie, ETH Zentrum, 8092 Zürich, Switzerland*

Received July 30, 1997; revised October 15, 1997

**A zero-quantum/double-quantum HNCO(H) constant time experiment is presented for the quantitative evaluation of dipole–CSA cross-correlated relaxation involving the $^{1}H^{N}$, $^{15}N$, and $^{13}C'$ nuclei of the peptide plane. A simple procedure that allows the extraction of cross-correlated relaxation rate constants from intensity ratios of well-resolved doublet components along $\omega_1$ is described. The experiment is demonstrated on fully $^{13}C$, $^{15}N$-labeled ubiquitin.** © 1998 Academic Press

*Key Words:* **nuclear spin relaxation; dipole–CSA cross-correlated relaxation; ZQ/DQ spectroscopy; chemical shielding anisotropy; protein backbone dynamics; anisotropic motion.**

---

The potential of nuclear spin cross-correlated relaxation as a source of structural and dynamic information in biomolecules, complementing the standard $T_1$, $T_2$, NOE relaxation parameters, was recognized some time ago (*1–5*). In particular, magnetic dipole–dipole and dipole–CSA (chemical shielding anisotropy) cross-correlation parameters provide information about dihedral angles, CSA tensors, and anisotropic intramolecular and overall tumbling motion. However, in the past quantitative determination of cross-correlation rate constants required a large experimental effort and often accurate knowledge of scalar *J*-coupling constants, which did not stimulate widespread applications. Recently, new experiments were proposed, which are conceptually related to experiments for scalar *J*-coupling determination, allowing efficient measurements of heteronuclear cross-correlated relaxation rate constants in biomolecules (*6, 7*).

Here we present a general scheme for measuring cross-correlation-induced cross-relaxation effects in three-spin systems by using ZQ/DQ (zero-quantum/double-quantum) NMR experiments. ZQ/DQ experiments were previously applied for protein resonance assignment (*8, 9*), for *J*-coupling measurements (*10*), and for measuring dipole–dipole cross-correlated relaxation (*7*). We show here that this class of experiments can also be used for the quantitative extraction of various dipole–CSA cross-correlation rate constants including some rate constants which are otherwise difficult to assess. The method is demonstrated for the three-spin system consisting of the $^{1}H^{N}$, $^{15}N$, and $^{13}C'$ nuclei of the peptide plane in proteins. A key feature of the experiment is that the cross-correlated relaxation effects of interest are manifested as differential monoexponential relaxation in the two components of the normally well-resolved $^{15}N-^{1}H^{N}$ doublet. This allows a simple and robust procedure for the extraction of cross-correlation parameters, which is well suited to practical applications.

Most NMR studies on peptide-plane dynamics focus on $\{^{1}H\}^{15}N$-NOE data and on $T_1$, $T_2$ autorelaxation measurements of $^{15}N$ nuclei (*11*) and more recently also of carbonyl $^{13}C'$ nuclei (*12*). Because of the rigidity of the peptide plane the combined use of all these parameters helps one to derive a more realistic picture of peptide-plane motions in terms of locally isotropic or anisotropic reorientational fluctuations (*13*). It is shown here that dipole–CSA cross-correlated relaxation rate constants provide additional independent information toward this goal.

The proposed ZQ/DQ HNCO(H) experiment is depicted in Fig. 1 with the central building block CT as a constant-time period of length $T$. At the beginning of this block transverse two-spin $^{15}N$, $^{13}C'$ terms $C_xN_x$, $C_xN_y$ are present in the spin-density operator that can be decomposed into ZQ coherences $C_+N_-$, $C_-N_+$ and DQ coherences $C_+N_+$, $C_-N_-$. They experience during the time $T$ auto- and cross-correlated relaxation together with chemical shift and scalar *J*-coupling evolution. The ZQ/DQ HNCO(H) experiment of Fig. 1 is a 2D experiment, but the CT building block can easily be incorporated into experiments of higher dimensions. The sum $\Gamma$ of cross-correlation rate constants is obtained in a straightforward manner from the intensity ratio of the peak doublet components along $\omega_1$ using $\Gamma = (2T)^{-1}\ln\{I_2(T)/I_1(T)\}$.

This and other relationships are derived in the following by considering the weakly coupled three-spin $\frac{1}{2}$ system $^{1}H^{N}$ $^{15}N$ $^{13}C'$ spins of the peptide plane with the static Hamiltonian $H_0$

$$H_0 = \omega_H H_z + \omega_N N_z + \omega_C C_z + 2\pi {}^1J_{NH} H_z N_z + 2\pi {}^2J_{CH} H_z C_z + 2\pi {}^1J_{NC} C_z N_z, \quad [1]$$



1090-7807/98 $25.00
Copyright © 1998 by Academic Press
All rights of reproduction in any form reserved.

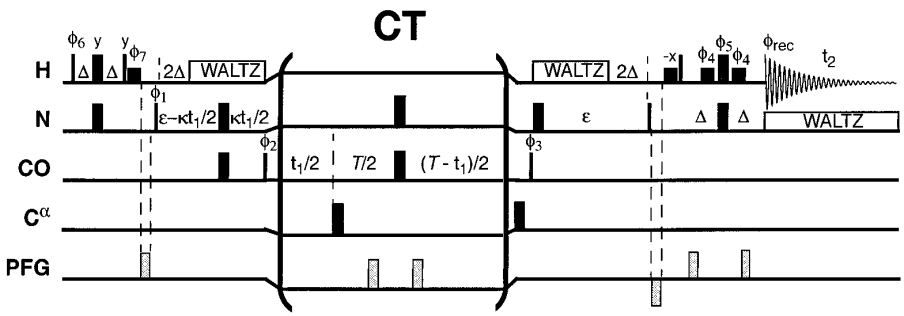


**FIG. 1.** Pulse sequence of the 2D ZQ/DQ HNCO(H) constant time experiment for dipole–CSA cross-correlated relaxation measurements of the peptide plane of $^{15}$N, $^{13}$C-labeled proteins. Cross-correlated relaxation is monitored during the constant delay $T$, highlighted in the pulse sequence. $^{15}$N quadrature detection along $t_1$ is achieved by incrementing $\phi_1$ according to the TPPI–States method. Two peak doublets are obtained per residue at the positions $\omega^{ZQ} = (1 + \kappa)\omega_N - \omega_C \pm \pi J^{ZQ}$ and $\omega^{DQ} = (1 + \kappa)\omega_N + \omega_C \pm \pi J^{DQ}$. Alternatively, $\phi_2$ can be incremented for C′ quadrature detection resulting in a spectrum with the peak doublets at positions $\omega^{ZQ} = \omega_C - (1 + \kappa)\omega_N \pm \pi J^{ZQ}$ and $\omega^{DQ} = \omega_C + (1 + \kappa)\omega_N \pm \pi J^{DQ}$. The parameter $\kappa$ can be adjusted in the range $0 \leq \kappa \leq (\epsilon - 2\Delta)/t_1^{max}$ to minimize spectral overlaps. All RF pulses without a phase label are applied along the $x$ axis. Selective water flipback pulses are used with a rectangular shape and a RF-field strength of $|\gamma B_1|/(2\pi) = 250$ Hz. Pulsed field gradients are inserted as indicated for coherence-transfer pathway selection and residual water suppression. $^1$H and $^{15}$N composite pulse decoupling is achieved using WALTZ-16 with $|\gamma B_1|/(2\pi) = 4$ and 1 kHz, respectively. The transfer delays $\Delta$ and $\epsilon$ are set to $\Delta \cong 1/(4J_{NH})$ and $\epsilon \cong 1/(2J_{NC})$. Phase cycling is as follows: $\phi_1 = 8(x, -x)$, $\phi_2 = 2(x, x, x, x, -x, -x, -x, -x)$, $\phi_4 = -\phi_5 = 4(x, x, -x, -x)$, $\phi_6 = -\phi_7 = 8x, 8(-x)$, $\phi_{rec} = 2(x, -x), 4(-x, x), 2(x, -x)$.

where $\omega_H$, $\omega_N$, and $\omega_C$ are the Larmor frequencies of the spins involved; $^1J_{NH}$, $^2J_{CH}$, and $^1J_{NC}$ are the scalar $J$-coupling constants between the three spins; and the spin operators are denoted by the respective element letters. The master equation, which governs the spin dynamics, has a block-diagonal matrix representation with respect to the ZQ and DQ manifolds spanned by the operators $B_1^{ZQ} = \frac{1}{2}N_+C_- + N_+C_-H_z^N$, $B_2^{ZQ} = \frac{1}{2}N_+C_- - N_+C_-H_z^N$ and $B_1^{DQ} = \frac{1}{2}N_+C_+ + N_+C_+H_z^N$, $B_2^{DQ} = \frac{1}{2}N_+C_+ - N_+C_+H_z^N$ (the conjugate manifolds transform correspondingly):

$$\frac{d}{dt}\mathbf{b}^{ZQ} = -\begin{pmatrix} i\pi J^{ZQ} + \dfrac{\Gamma_{in}^{ZQ} + \Gamma_{anti}^{ZQ}}{2} + \Gamma^{ZQ} & \dfrac{\Gamma_{in}^{ZQ} - \Gamma_{anti}^{ZQ}}{2} \\ \dfrac{\Gamma_{in}^{ZQ} - \Gamma_{anti}^{ZQ}}{2} & -i\pi J^{ZQ} + \dfrac{\Gamma_{in}^{ZQ} + \Gamma_{anti}^{ZQ}}{2} - \Gamma^{ZQ} \end{pmatrix}\mathbf{b}^{ZQ} - i(\omega_N - \omega_C)\mathbf{b}^{ZQ} \qquad [2]$$

$$\frac{d}{dt}\mathbf{b}^{DQ} = -\begin{pmatrix} i\pi J^{DQ} + \dfrac{\Gamma_{in}^{DQ} + \Gamma_{anti}^{DQ}}{2} + \Gamma^{DQ} & \dfrac{\Gamma_{in}^{DQ} - \Gamma_{anti}^{DQ}}{2} \\ \dfrac{\Gamma_{in}^{DQ} - \Gamma_{anti}^{DQ}}{2} & -i\pi J^{DQ} + \dfrac{\Gamma_{in}^{DQ} + \Gamma_{anti}^{DQ}}{2} - \Gamma^{DQ} \end{pmatrix}\mathbf{b}^{DQ} - i(\omega_N + \omega_C)\mathbf{b}^{DQ}. \qquad [3]$$

The coefficients $b_1^{ZQ}$ and $b_2^{ZQ}$ are proportional to the peak volumes of the ZQ doublet components that are separated in the spectrum by $2\pi J^{ZQ}$, and $b_1^{DQ}$ and $b_2^{DQ}$ are proportional to the corresponding volumes of the DQ doublet. $\Gamma_{in}^{ZQ}$, $\Gamma_{anti}^{ZQ}$, $\Gamma_{in}^{DQ}$, and $\Gamma_{anti}^{DQ}$ are the autorelaxation rate constants of the in-phase and antiphase ZQ and DQ operators $N_+C_- = B_1^{ZQ} + B_2^{ZQ}$, $2N_+C_-H_z^N = B_1^{ZQ} - B_2^{ZQ}$, $N_+C_+ = B_1^{DQ} + B_2^{DQ}$, and $2N_+C_+H_z^N = B_1^{DQ} - B_2^{DQ}$. The scalar $J$-coupling constants and the cross-correlated relaxation rate constants entering Eqs. [2] and [3] are

The coefficient vectors $\mathbf{b}^{ZQ}$ and $\mathbf{b}^{DQ}$ represent the ZQ and DQ components of the spin-density operator $\sigma$

$$\mathbf{b}^{ZQ} = \begin{pmatrix} b_1^{ZQ} \\ b_2^{ZQ} \end{pmatrix} = \begin{pmatrix} \mathrm{Tr}\{B_1^{ZQ\dagger}\sigma\} \\ \mathrm{Tr}\{B_2^{ZQ\dagger}\sigma\} \end{pmatrix}$$

$$\text{and} \quad \mathbf{b}^{DQ} = \begin{pmatrix} b_1^{DQ} \\ b_2^{DQ} \end{pmatrix} = \begin{pmatrix} \mathrm{Tr}\{B_1^{DQ\dagger}\sigma\} \\ \mathrm{Tr}\{B_2^{DQ\dagger}\sigma\} \end{pmatrix}. \qquad [4]$$

$$J^{ZQ} = {}^1J_{NH} - {}^2J_{CH} \qquad [5]$$

$$J^{DQ} = {}^1J_{NH} + {}^2J_{CH} \qquad [6]$$

$$\Gamma^{ZQ} = \Gamma_{N,NH} + \Gamma_{C,CH} - \Gamma_{N,CH} - \Gamma_{C,NH} \qquad [7]$$

$$\Gamma^{DQ} = \Gamma_{N,NH} + \Gamma_{C,CH} + \Gamma_{N,CH} + \Gamma_{C,NH}. \qquad [8]$$

$\Gamma_{I,SW}$ denotes a CSA–dipole cross-correlation rate constant with respect to the CSA interaction of spin $I$ and the dipolar

interaction between spins $S$ and $W$. Dipole–dipole cross-correlated relaxation and cross-correlation effects involving the $H^N$ CSA interaction affect neither $\Gamma^{ZQ}$ nor $\Gamma^{DQ}$.

For $W = I$, which applies to $\Gamma_{N,NH}$ and $\Gamma_{C,CH}$,

$$\Gamma_{I,IS} = -\tfrac{1}{30}\gamma_I B_0 \xi_{IS}\{\sigma_x[4J_{d,x}(0) + 3J_{d,x}(\omega_I)] + \sigma_y[4J_{d,y}(0) + 3J_{d,y}(\omega_I)]\}, \quad [9]$$

and for $W \neq I$, which applies to $\Gamma_{N,CH}$ and $\Gamma_{C,NH}$,

$$\Gamma_{I,SW} = -\tfrac{1}{30}\gamma_I B_0 \xi_{SW}\{\sigma_x 4J_{d,x}(0) + \sigma_y 4J_{d,y}(0)\}, \quad [10]$$

where $B_0$ is the magnetic field strength, $\gamma_I$ is the gyromagnetic ratio of spin $I$, $\xi_{IS} = (\mu_0/4\pi)\hbar\gamma_I\gamma_S\langle r_{IS}^{-3}\rangle$, and $r_{IS}$ is the distance between spins $I$ and $S$. $\sigma_x$ and $\sigma_y$ depend on the principal values $\sigma_{xx}$, $\sigma_{yy}$, $\sigma_{zz}$ ($\sigma_{xx} + \sigma_{yy} + \sigma_{zz} = 0$) of the CSA tensor of spin $I$: $\sigma_x = \sigma_{xx} - \sigma_{zz}$ and $\sigma_y = \sigma_{yy} - \sigma_{zz}$. The power spectral density functions $J_{d,x}(\omega)$ and $J_{d,y}(\omega)$ are the Fourier transforms of the cross-correlation functions between the principal axes $x$ and $y$ of the CSA tensor and the dipolar director (index d). Equation [10] is an extension for a non-axially symmetric CSA tensor of the corresponding expression of Ref. (*5*). Equations [9] and [10] are valid for arbitrary permutations of the CSA axis labels. Since the CSA interaction and the dipolar interaction entering $\Gamma_{I,SW}$ of Eq. [10] are not required to be in spatial proximity, $\Gamma_{I,SW}$ was previously termed ''remote cross correlation'' (*14*). A dipole–dipole cross-correlation analogue was described in Ref. (*7*).

For isotropic overall rotational tumbling with the correlation time $\tau_c$ and local fluctuations in the extreme narrowing limit ($\tau_{int}\omega_0 \ll 1$), the power spectral density entering Eqs. [9] and [10] can be expressed in a model-free way (*15, 16*),

$$J_{d,\mu}(\omega) = \frac{2S_{d,\mu}^2\tau_c}{1 + (\omega\tau_c)^2} + \frac{2(P_2(\cos\chi_{d,\mu}) - S_{d,\mu}^2)\tau_{eff}}{1 + (\omega\tau_{eff})^2}, \quad [11]$$

where $P_2(x) = (3x^2 - 1)/2$. The effective correlation time $\tau_{eff}$ is given by $\tau_{eff}^{-1} = \tau_c^{-1} + \tau_{int}^{-1}$ and $\chi_{d,\mu}$ is the angle between the CSA principal axis $\Omega_\mu$ ($\mu = x, y, z$) and the dipolar director $\Omega_d$. The generalized order parameter is

$$S_{d,\mu}^2 = \frac{4\pi}{5}\sum_{m=-2}^{2}\langle Y_{2m}(\Omega_d)\rangle\langle Y_{2m}^*(\Omega_\mu)\rangle, \quad [12]$$

where $Y_{2m}(\Omega)$ are the normalized second-order spherical harmonics.

If $|2\pi J^{ZQ}| \gg |\Gamma_{in}^{ZQ} - \Gamma_{anti}^{ZQ}|/2$ and $|2\pi J^{DQ}| \gg |\Gamma_{in}^{DQ} - \Gamma_{anti}^{DQ}|/2$ in Eqs. [2] and [3], the secular approximation can be applied (*17*), i.e., the off-diagonal elements can be neglected, leading in the absence of RF pulses to the following simple ZQ evolution:

$$b_{1,2}^{ZQ}(t) = \exp\{-i(\omega_N - \omega_C \pm \pi J^{ZQ})t\} \times \exp\left\{-\left(\frac{(\Gamma_{in}^{ZQ} + \Gamma_{anti}^{ZQ})}{2} \pm \Gamma^{ZQ}\right)t\right\} b_{1,2}^{ZQ}(0). \quad [13]$$

An analogous expression is valid for DQ evolution. Since $J^{ZQ}$ and $J^{DQ}$ are dominated by the $^1J_{NH}$ coupling ($|^1J_{NH}| \approx$ 94 Hz and $|^2J_{CH}| \approx 2$–$5$ Hz), the secular approximation is well fulfilled for the system considered here. Note that in the absence of scalar $J$-coupling evolution, realized, e.g., by spin-lock experiments (*16*), the ''secular'' condition is usually more stringent $|\Gamma^{ZQ/DQ}| \gg |\Gamma_{in}^{ZQ/DQ} - \Gamma_{anti}^{ZQ/DQ}|/2$. If this condition is not fulfilled the relaxation becomes multiexponential.

The experiment of Fig. 1 is of the ZQ/DQ HNCO type (*9*) with a constant time (CT) element inserted. This scheme allows separation of the oscillatory terms in Eq. [13] from the ''dissipative'' $\Gamma$ terms. During the CT period no RF pulses are applied on the $^1$H spins such that cross-correlated relaxation can occur during the total time $T$. After Fourier transformation, cross-correlated relaxation manifests itself only in the intensity of the doublet lines, but not in their linewidth. As in other CT experiments the linewidth is determined by apodization and by the inhomogeneity of the magnetic field. Line splitting due to the scalar coupling with $C^\alpha$ spins is removed by a selective 180° pulse on the $C^\alpha$ spins.

The intensities of the doublet components (separated by the scalar couplings $J^{ZQ}$ and $J^{DQ}$, respectively) decay monoexponentially with $T$,

$$I_{1,2}^{ZQ}(T) \propto b_{1,2}^{ZQ}(T) = \exp\left(-\left(\frac{\Gamma_{in}^{ZQ} + \Gamma_{anti}^{ZQ}}{2} \pm \Gamma^{ZQ}\right)T\right) b_{1,2}^{ZQ}(0), \quad [14]$$

and the analogous expression applies to $I_{1,2}^{DQ}(T) \propto b_{1,2}^{DQ}(T)$. The desired cross-correlated relaxation rate constants $\Gamma^{ZQ}$ and $\Gamma^{DQ}$ can then be directly extracted from the intensity ratios at a single mixing time $T$:

$$\Gamma^{ZQ} = \frac{1}{2T}\ln\left(\frac{I_2^{ZQ}(T)}{I_1^{ZQ}(T)}\right) \quad \text{and} \quad \Gamma^{DQ} = \frac{1}{2T}\ln\left(\frac{I_2^{DQ}(T)}{I_1^{DQ}(T)}\right). \quad [15]$$

Finally, linear combination of $\Gamma^{ZQ}$ and $\Gamma^{DQ}$ leads according to Eqs. [7] and [8] to

$$\Gamma^{local} = \Gamma_{N,NH} + \Gamma_{C,CH} = \tfrac{1}{2}(\Gamma^{DQ} + \Gamma^{ZQ}) \quad [16]$$

$$\Gamma^{\text{remote}} = \Gamma_{\text{N,CH}} + \Gamma_{\text{C,NH}} = \tfrac{1}{2}(\Gamma^{\text{DQ}} - \Gamma^{\text{ZQ}}). \quad [17]$$

Thus, the ZQ/DQ experiment yields the sum of ''symmetric'' pairs of CSA–dipole cross-correlated rate constants. $\Gamma^{\text{local}}$ can be further decomposed by measuring $\Gamma_{\text{N,NH}}$ or $\Gamma_{\text{C,CH}}$ from single-quantum experiments (*6*), whereas $\Gamma^{\text{remote}}$ is more difficult to decompose and is best directly interpreted.

The effect of additional spins on the measured cross-correlated relaxation rate constants has been estimated by including a $H^{\alpha}$ or a $C^{\alpha}$ spin as a fourth spin in the master equation and by simulating the decay of ZQ/DQ doublets.

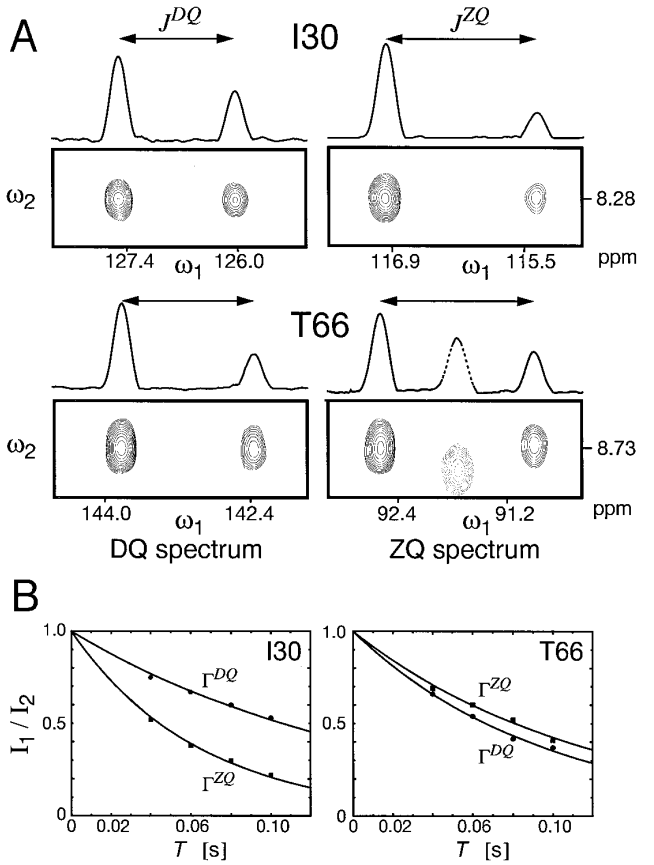


**FIG. 2.** Experimental results of the 2D ZQ/DQ HNCO(H) experiment of Fig. 1 applied to human ubiquitin at 300 K and 14.1 T $B_0$-field strength. Quadrature detection on $^{15}$N was used in $\omega_1$ and the $^{13}$C′ demodulation frequency was shifted to 182.5 ppm by time-proportional phase incrementation of $\phi_3$. The parameter $\kappa$ was set to $\kappa = 0$. In A, contour plots of ZQ and DQ cross-peak doublets are shown for the peptide plane between Lys 29 and Ile 30 and between Ser 65 and Thr 66 with $T = 80$ ms, where $\omega_1$ corresponds to the ZQ/DQ dimension and $\omega_2$ to the $H^N$ frequency. Projections are drawn along the cross-correlated relaxation-active ZQ/DQ frequency domain $\omega_1$ ($^{15}$N ppm scale). Peak intensities were fitted to the function of Eq. (15) as shown in B for relaxation delays $T = 40$, 60, 80, and 100 ms. The extracted cross-correlation rate constants are for the peptide plane between Lys 29 and Ile 30 $\Gamma^{\text{local}} = 5.7 \pm 0.2\ \text{s}^{-1}$ and $\Gamma^{\text{remote}} = -2.3 \pm 0.2\ \text{s}^{-1}$ and for that connecting Ser 65 with Thr 66 $\Gamma^{\text{local}} = 4.8 \pm 0.2\ \text{s}^{-1}$ and $\Gamma^{\text{remote}} = 0.4 \pm 0.2\ \text{s}^{-1}$, respectively.

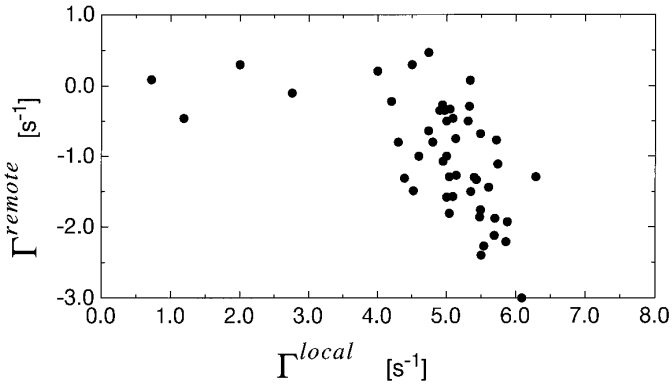


**FIG. 3.** Experimental cross-correlation rate constants $\Gamma^{\text{remote}}$ vs $\Gamma^{\text{local}}$ (see Eqs. [16] and [17]) of 48 peptide planes of ubiquitin recorded with the pulse sequence of Fig. 1 under the conditions given in Fig. 2.

The values of $\Gamma^{\text{ZQ}}$ and $\Gamma^{\text{DQ}}$ determined from these simulations on the basis of Eqs. [15]–[17] show that the influence of additional spins can be neglected in good approximation as they almost equally affect the doublet components. Thus, the proposed HNCO(H) experiment offers a convenient way to determine the above cross-correlation rate constants without any assumption being made about additional relaxation contributions or unresolved scalar $J$ couplings that in other cross-correlation experiments tend to complicate the interpretation (*5*). These types of cross-correlation parameters have the advantage over standard $T_2$ and $T_{1\rho}$ parameters that they are independent of slow conformational exchange (*18*) provided that the scalar $J$ couplings involved are not modulated (*16*).

The 2D ZQ/DQ HNCO(H) experiment of Fig. 1 was applied to human ubiquitin, a small globular protein with an isotropic rotational tumbling correlation time $\tau_c = 4.1$ ns at 300 K (*19, 20*). Examples of ZQ and DQ peak doublets along $\omega_1$ are shown in Fig. 2. The cross-correlated relaxation rate constants were extracted by fitting Eq. [15] to the peak intensity ratios obtained for different relaxation delays $T$. All peak intensities follow, within the experimental accuracy, a monoexponential decay as a function of $T$, which is consistent with the theoretical prediction of Eq. [14]. The cross-correlated relaxation effects are exemplified with the two peptide planes connecting residue Lys 29 with residue Ile 30 (plane 1) and Ser 65 with Thr 66 (plane 2). For plane 1 dipole–CSA cross correlation for the ZQ coherence is considerably more effective than that for the DQ coherence, while for plane 2 the two relaxation rates are similar with a slightly smaller effect for the ZQ coherence. This results in a different sign of the remote cross-correlated relaxation rate constants $\Gamma^{\text{remote}}$ for the two residues. The experimental $\Gamma^{\text{local}}$ and $\Gamma^{\text{remote}}$ values of these two peptide planes are given in the legend to Fig. 2.

Using the experiment of Fig. 1, the cross-correlated relaxation rate constants $\Gamma^{\text{local}}$ and $\Gamma^{\text{remote}}$ could be measured for

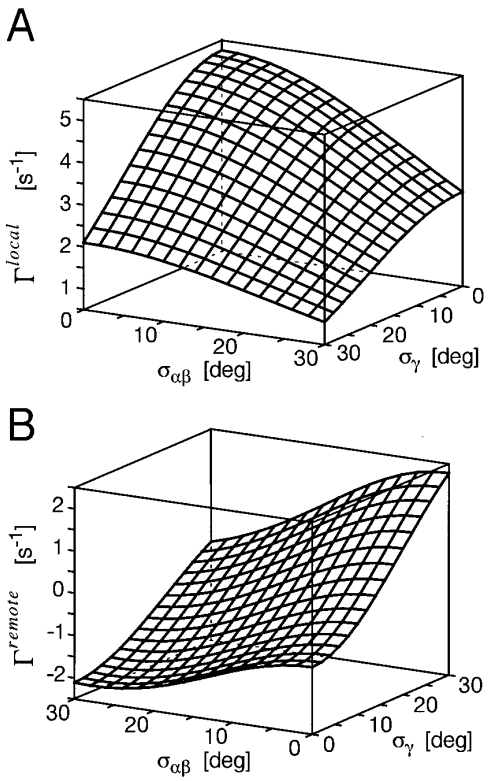


**FIG. 4.** Dependence of cross-correlation terms $\Gamma^{local}$ (A) and $\Gamma^{remote}$ (B) on internal anisotropic reorientational fluctuations of the peptide plane as described by the 3D GAF model (*13*) assuming $\omega_0\tau_{int} \ll 1$. The rate constants are calculated for an overall tumbling correlation time $\tau_c = 4.1$ ns and a static $B_0$ magnetic field of 14.1 T. The fluctuation was assumed to be axially symmetric with the symmetry axis $\gamma$ parallel to the $C^\alpha_{i-1}$–$C^\alpha_i$ vector. The axial fluctuation amplitudes $\sigma_{\alpha\beta} = \sigma_\alpha = \sigma_\beta$ and $\sigma_\gamma$ were varied between 0° and 30°. Standard bond geometries of the peptide plane were assumed (*21*) and the CSA parameters were taken from Refs. (*22, 23*).

48 peptide planes in ubiquitin with the distribution of $\Gamma^{local}$ and $\Gamma^{remote}$ shown in Fig. 3. $\Gamma^{local}$ varies between 0.7 and 6.3 $s^{-1}$, whereas $\Gamma^{remote}$ varies between $-3.0$ and 0.5 $s^{-1}$. The four smallest $\Gamma^{local}$ values belong to peptide planes of the flexible C-terminus. The rather weak overall correlation between $\Gamma^{local}$ and $\Gamma^{remote}$ indicates that these two cross-correlation parameters carry complementary information about CSA tensors and about anisotropic internal and overall motion.

The effect of anisotropic internal reorientational Gaussian motion of the peptide plane described by the 3D GAF model (*13*) on cross-correlation rate constants of $\Gamma^{local}$ and $\Gamma^{remote}$ is illustrated in Fig. 4 for $\tau_c = 4.1$ ns assuming standard bonding geometries (*21*), $^{13}C'$ and $^{15}N$ CSA parameters from Refs. (*22, 23*), and fast internal time scales $\omega_0\tau_{int} \ll 1$. The dependence of the rate constants on the internal reorientational fluctuation amplitudes $\sigma_\alpha$, $\sigma_\beta$, $\sigma_\gamma$ about the three orthogonal axes $\alpha$, $\beta$, $\gamma$ attached to the peptide plane is shown. The $\gamma$ axis was chosen along the $C^\alpha_{i-1}$–$C^\alpha_i$ vector and $\sigma_\alpha = \sigma_\beta = \sigma_{\alpha\beta}$ was assumed, which was found in molecular dynamics simulations often to be the case (*13*). The principal axes of the various spin interactions probe the reorientational fluctuations about the various axes differently as is reflected in the distinct behavior of $\Gamma^{local}$ and $\Gamma^{remote}$ as functions of the $\sigma_{\alpha\beta}$ and $\sigma_\gamma$ fluctuation amplitudes. While an increase of $\sigma_{\alpha\beta}$ and $\sigma_\gamma$ leads to a reduction of $\Gamma^{local}$, $\sigma_{\alpha\beta}$ and $\sigma_\gamma$ have an opposite influence on $\Gamma^{remote}$. The two cross-correlation parameters have a similar dynamic range, but only $\Gamma^{remote}$ crosses zero for realistic fluctuation amplitudes. Most experimental values of Fig. 3 lie inside the range covered by the simulated cross-correlation parameters of Fig. 4, despite the fact that the CSA tensors involved may significantly deviate from the standard values (*22, 23*) underlying Fig. 4.

In conclusion, the CT pulse-sequence element of Fig. 1 is well suited to measuring dipole–CSA cross-correlated relaxation via multiple-quantum coherences. Its application is not restricted to the HNCO(H) experiment presented here and it can be inserted into other 2D and 3D heteronuclear transfer experiments to quantitatively measure heteronuclear cross-correlated relaxation processes. A study is currently under way in our group that explores the practical use of these relaxation parameters in combination with standard autorelaxation parameters to characterize local and global isotropic and anisotropic protein dynamics.

## ACKNOWLEDGMENTS

Helpful discussions with Stephan Lienin are acknowledged. B.B. is a recipient of an EMBO fellowship and N.R.S. is a recipient of an NSERC scholarship (Canada). This work was supported by the Swiss National Science Foundation.

## REFERENCES

1. L. G. Werbelow and D. M. Grant, *Adv. Magn. Reson.* **9,** 189 (1977).
2. T. E. Bull, *J. Magn. Reson.* **72,** 397 (1987).
3. C. Dalvit and G. Bodenhausen, *J. Am. Chem. Soc.* **110,** 7924 (1988).
4. R. Brüschweiler, C. Griesinger, and R. R. Ernst, *J. Am. Chem. Soc.* **111,** 8034 (1989).
5. J. Boyd, U. Hommel, and V. V. Krishnan, *Chem. Phys. Lett.* **187,** 317 (1991).
6. N. Tjandra, A. Szabo, and A. Bax, *J. Am. Chem. Soc.* **118,** 6986 (1996); A. Bax, Experimental NMR Conference, oral contribution, Florida, 1997.
7. B. Reif, M. Hennig, and C. Griesinger, *Science* **276,** 1230 (1997).
8. T. Szyperski, G. Wider, J. H. Bushweller, and K. Wüthrich, *J. Am. Chem. Soc.* **115,** 9307 (1993).
9. B. Brutscher, J.-P. Simorre, M. Caffrey, and D. Marion, *J. Magn. Reson. B* **105,** 77 (1994).
10. A. Rexroth, P. Schmidt, S. Szalma, T. Geppert, H. Schwalbe, and C. Griesinger, *J. Am. Chem. Soc.* **117,** 10389 (1995).
11. L. E. Kay, D. A. Torchia, and A. Bax, *Biochemistry* **28,** 8972 (1989).
12. J. Engelke and H. Rüterjans, *J. Biomol. NMR* **9,** 163 (1997).

*13.* T. Bremi and R. Brüschweiler, *J. Am. Chem. Soc.* **119,** 6672 (1997).

*14.* P. Kumar and A. Kumar, *J. Magn. Reson. A* **119,** 29 (1996).

*15.* G. Lipari and A. Szabo, *J. Am. Chem. Soc.* **104,** 4546, 4559 (1982).

*16.* R. Brüschweiler and R. R. Ernst, *J. Chem. Phys.* **96,** 1758 (1992).

*17.* M. Goldman, *J. Magn. Reson.* **60,** 437 (1984).

*18.* B. Brutscher, R. Brüschweiler, and R. R. Ernst, *Biochemistry* **36,** 13043 (1997).

*19.* D. M. Schneider, M. J. Dellwo, and J. A. Wand, *Biochemistry* **31,** 3645 (1992).

*20.* N. Tjandra, E. S. Feller, R. Pastor, and A. Bax, *J. Am. Chem. Soc.* **117,** 12562 (1995).

*21.* T. E. Creighton, ''Proteins,'' Freeman, New York (1984).

*22.* C. J. Hartzell, M. Whitfield, T. G. Oas, and G. P. Drobny, *J. Am. Chem. Soc.* **109,** 5966 (1987).

*23.* Y. Hiyama, C.-H. Niu, J. V. Silverton, A. Bavoso, and D. A. Torchia, *J. Am. Chem. Soc.* **110,** 2378 (1988).